The Electronic Supplementary Information (ESI) of "Improved Model on Fluorescence Decay in Singlet Fission Materials"

Fang-qi Hu
Center for quantum technology research, School of Physics, Beijing Institute of Technology, Beijing 100081, People's Republic of China and China Academy of Engineering Physics, Beijing 100088, People's Republic of China

Qing Zhao and Xu-biao Peng*
Center for quantum technology research, School of Physics, Beijing Institute of Technology, Beijing 100081, People's Republic of China

ESI A: The matrix form of total Hamiltonian

The representation of total spin Hamiltonian Eq. (5) in text under ordered basis $|x_a x_b\rangle$, $|x_a y_b\rangle$, $\cdots$, $|z_a z_b\rangle$ has five parts and is presented in the following. The Zeeman splitting term $H_{\mathrm{Ze,a}}$ of molecule **a**:

$$ig\beta B\begin{pmatrix} 0 & 0 & 0 & 1 & 0 & 0 & 0 & 0 & 0 \\ 0 & 0 & 0 & 0 & 1 & 0 & 0 & 0 & 0 \\ 0 & 0 & 0 & 0 & 0 & 1 & 0 & 0 & 0 \\ -1 & 0 & 0 & 0 & 0 & 0 & 0 & 0 & 0 \\ 0 & -1 & 0 & 0 & 0 & 0 & 0 & 0 & 0 \\ 0 & 0 & -1 & 0 & 0 & 0 & 0 & 0 & 0 \\ 0 & 0 & 0 & 0 & 0 & 0 & 0 & 0 & 0 \\ 0 & 0 & 0 & 0 & 0 & 0 & 0 & 0 & 0 \\ 0 & 0 & 0 & 0 & 0 & 0 & 0 & 0 & 0 \end{pmatrix}. \tag{A1}$$

The Zeeman splitting term $H_{\mathrm{Ze,b}}$ of molecule **b**:

$$ig\beta B\begin{pmatrix} 0 & 1 & 0 & 0 & 0 & 0 & 0 & 0 & 0 \\ -1 & 0 & 0 & 0 & 0 & 0 & 0 & 0 & 0 \\ 0 & 0 & 0 & 0 & 0 & 0 & 0 & 0 & 0 \\ 0 & 0 & 0 & 0 & 1 & 0 & 0 & 0 & 0 \\ 0 & 0 & 0 & -1 & 0 & 0 & 0 & 0 & 0 \\ 0 & 0 & 0 & 0 & 0 & 0 & 0 & 0 & 0 \\ 0 & 0 & 0 & 0 & 0 & 0 & 0 & 1 & 0 \\ 0 & 0 & 0 & 0 & 0 & 0 & -1 & 0 & 0 \\ 0 & 0 & 0 & 0 & 0 & 0 & 0 & 0 & 0 \end{pmatrix}. \tag{A2}$$

The zero-field splitting term $H_{\mathrm{zfs,a}}$ of molecule **a**:

$$\begin{aligned}
&H_{\mathrm{zfs,a}}(1,1) = H_{\mathrm{zfs,a}}(2,2) = H_{\mathrm{zfs,a}}(3,3) = \frac{1}{6}D[3\cos(2\theta_a) - 1] - E\cos^2(\theta_a)\cos(2\varphi_a), \\
&H_{\mathrm{zfs,a}}(1,4) = H_{\mathrm{zfs,a}}(4,1) = H_{\mathrm{zfs,a}}(2,5) = H_{\mathrm{zfs,a}}(5,2) = H_{\mathrm{zfs,a}}(3,6) = H_{\mathrm{zfs,a}}(6,3) = E\cos(\theta_a)\sin(2\varphi_a), \\
&H_{\mathrm{zfs,a}}(1,7) = H_{\mathrm{zfs,a}}(7,1) = H_{\mathrm{zfs,a}}(2,8) = H_{\mathrm{zfs,a}}(8,2) = H_{\mathrm{zfs,a}}(3,9) = H_{\mathrm{zfs,a}}(9,3) = \frac{1}{2}[D - E\cos(2\varphi_a)]\sin(2\theta_a), \\
&H_{\mathrm{zfs,a}}(4,7) = H_{\mathrm{zfs,a}}(7,4) = H_{\mathrm{zfs,a}}(5,8) = H_{\mathrm{zfs,a}}(8,5) = H_{\mathrm{zfs,a}}(6,9) = H_{\mathrm{zfs,a}}(9,6) = E\sin(\theta_a)\sin(2\varphi_a), \\
&H_{\mathrm{zfs,a}}(4,4) = H_{\mathrm{zfs,a}}(5,5) = H_{\mathrm{zfs,a}}(6,6) = \frac{D}{3} + E\cos(2\varphi_a), \\
&H_{\mathrm{zfs,a}}(7,7) = H_{\mathrm{zfs,a}}(8,8) = H_{\mathrm{zfs,a}}(9,9) = -E\cos(2\varphi_a)\sin^2(\theta_a) - \frac{1}{6}D[3\cos(2\theta_a) + 1],
\end{aligned} \tag{A3}$$

where the other elements are zero.

*Email: xubiaopeng@icloud.com

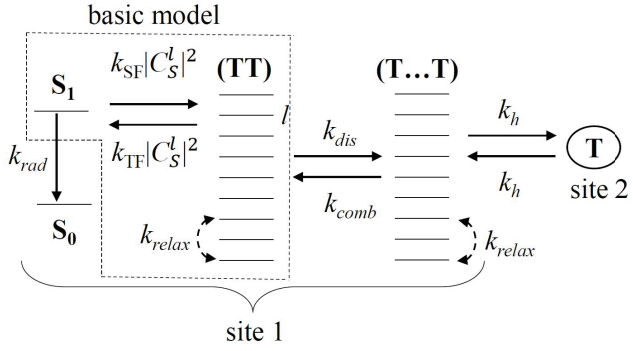

FIG. B1: Schematic representation of the simplified dynamic model.

The zero-field splitting term $H_{\mathrm{zfs,b}}$ of molecule **b**:

$$
\begin{aligned}
&H_{\mathrm{zfs,b}}(1,1) = H_{\mathrm{zfs,b}}(4,4) = H_{\mathrm{zfs,b}}(7,7) = \\
&\frac{1}{12}\{6\cos(2\theta_b)[D - E\cos(2\varphi_b)]\cos^2(\gamma_b) - [3\cos(2\gamma_b) - 1][D + 3E\cos(2\varphi_b)] + 12E\cos(\theta_b)\sin(2\gamma_b)\sin(2\varphi_b)\}, \\
&H_{\mathrm{zfs,b}}(2,2) = H_{\mathrm{zfs,b}}(5,5) = H_{\mathrm{zfs,b}}(8,8) = \\
&\frac{1}{12}\{6\cos(2\theta_b)[D - E\cos(2\varphi_b)]\sin^2(\gamma_b) + [3\cos(2\gamma_b) + 1][D + 3E\cos(2\varphi_b)] - 12E\cos(\theta_b)\sin(2\gamma_b)\sin(2\varphi_b)\}, \\
&H_{\mathrm{zfs,b}}(3,3) = H_{\mathrm{zfs,b}}(6,6) = H_{\mathrm{zfs,b}}(9,9) = -E\cos(2\varphi_b)\sin^2(\theta_b) - \frac{1}{6}D[3\cos(2\theta_b) + 1], \\
&H_{\mathrm{zfs,b}}(1,2) = H_{\mathrm{zfs,b}}(2,1) = H_{\mathrm{zfs,b}}(4,5) = H_{\mathrm{zfs,b}}(5,4) = H_{\mathrm{zfs,b}}(7,8) = H_{\mathrm{zfs,b}}(8,7) \\
&= \frac{1}{4}\{\{2D\sin^2(\theta_b) + [\cos(2\theta_b) + 3]E\cos(2\varphi_b)\}\sin(2\gamma_b) + 4E\cos(2\gamma_b)\cos(\theta_b)\sin(2\varphi_b)\}, \\
&H_{\mathrm{zfs,b}}(1,3) = H_{\mathrm{zfs,b}}(3,1) = H_{\mathrm{zfs,b}}(4,6) = H_{\mathrm{zfs,b}}(6,4) = H_{\mathrm{zfs,b}}(7,9) = H_{\mathrm{zfs,b}}(9,7) \\
&= \sin(\theta_b)\{\cos(\gamma_b)\cos(\theta_b)[D - E\cos(2\varphi_b)] + E\sin(\gamma_b)\sin(2\varphi_b)\}, \\
&H_{\mathrm{zfs,b}}(2,3) = H_{\mathrm{zfs,b}}(3,2) = H_{\mathrm{zfs,b}}(5,6) = H_{\mathrm{zfs,b}}(6,5) = H_{\mathrm{zfs,b}}(8,9) = H_{\mathrm{zfs,b}}(9,8) \\
&= \sin(\theta_b)\{[E\cos(2\varphi_b) - D]\cos(\theta_b)\sin(\gamma_b) + E\cos(\gamma_b)\sin(2\varphi_b)\},
\end{aligned}
\tag{A4}
$$

where the other elements are zero.

The exchange interaction term H_{ex}:

$$
X \begin{pmatrix}
0 & 0 & 0 & 0 & -1 & 0 & 0 & 0 & -1 \\
0 & 0 & 0 & 1 & 0 & 0 & 0 & 0 & 0 \\
0 & 0 & 0 & 0 & 0 & 0 & 1 & 0 & 0 \\
0 & 1 & 0 & 0 & 0 & 0 & 0 & 0 & 0 \\
-1 & 0 & 0 & 0 & 0 & 0 & 0 & 0 & -1 \\
0 & 0 & 0 & 0 & 0 & 0 & 0 & 1 & 0 \\
0 & 0 & 1 & 0 & 0 & 0 & 0 & 0 & 0 \\
0 & 0 & 0 & 0 & 0 & 1 & 0 & 0 & 0 \\
-1 & 0 & 0 & 0 & -1 & 0 & 0 & 0 & 0
\end{pmatrix}. \tag{A5}
$$

ESI B: The site independence of the dynamic model

Starting from Eqs. (14) where we assume that there are seven sites, we can simplify the model by summing over

both sides of Eqs. (14e-14j). As a result, we can get

$$\begin{aligned}
&\dot{N}_{\mathrm{S0}} = k_{\mathrm{rad}} N_{\mathrm{S1}} \\
&\dot{N}_{\mathrm{S1}} = -(k_{\mathrm{rad}} + k_{\mathrm{SF}}) N_{\mathrm{S1}} + k_{\mathrm{TF}} \sum_{l=1}^{9} |C_{\mathrm{S}}^{l}|^2 N_{(\mathrm{TT})l} \\
&\dot{N}_{(\mathrm{TT})l} = k_{\mathrm{SF}} |C_{\mathrm{S}}^{l}|^2 N_{\mathrm{S1}} - (k_{\mathrm{TF}} |C_{\mathrm{S}}^{l}|^2 + k_{\mathrm{dis}} + k_{\mathrm{relax}}) N_{(\mathrm{TT})l} + \sum_{j \neq l} \frac{1}{8} k_{\mathrm{relax}} N_{(\mathrm{TT})j} + k_{\mathrm{comb}} N_{(\mathrm{T\ldots T})l} \\
&\dot{N}_{(\mathrm{T\ldots T})l} = k_{\mathrm{dis}} N_{(\mathrm{TT})l} - (k_{\mathrm{comb}} + \frac{k_{\mathrm{h}}}{9} + k_{\mathrm{relax}}) N_{(\mathrm{T\ldots T})l} + \sum_{j \neq l} \frac{1}{8} k_{\mathrm{relax}} N_{(\mathrm{T\ldots T})j} + k_{\mathrm{h}} N_{\mathrm{T1}} \\
&\sum_{i=1}^{6} \dot{N}_{\mathrm{T,i}} = \frac{k_{\mathrm{h}}}{9} \sum_{l=1}^{9} N_{(\mathrm{T\ldots T})l} - k_{\mathrm{h}} N_{\mathrm{T1}}
\end{aligned} \tag{B1}$$

Clearly, all the above equations are independent of the number of sites except the left hand side of the last equation. However, note that there is a relation $\dot{N}_{\mathrm{S0}} + \dot{N}_{\mathrm{S1}} + \sum_{l=1}^{9}(\dot{N}_{(\mathrm{TT})l} + \dot{N}_{(\mathrm{T\ldots T})l}) + \sum_{i=1}^{6} \dot{N}_{\mathrm{T,i}} = 0$, and hence the left sides of the equations are also independent of the number of sites. As a result, we can see all the equations of our dynamic model are independent of the number of site and the model can be simplified to FIG .B1.

ESI C: The effects of the various rates in the extended model on FD

The effects of all rate constants on fluorescence dynamics are investigated by our extended dynamic model Eqs. (14) under Hamiltonian Eq. (5) for magnetic random in the presence of high field $B = 0.81$, as shown in FIG. C1. Since the effects of the rate constants on the singlet state decay rate $\ln(k_{\mathrm{NS0}})$ and on SF rate $\ln(k_{\mathrm{NTT}})$ are similar, here we only show the evolutions of $\ln(k_{\mathrm{NS0}})$ and $\ln(k_{\mathrm{NS1}})$. It can be seen in FIG. C1(a, b) that the prompt fluorescence is impaired and the delayed fluorescence is strengthened as the rate of SF k_{SF} increases and/or the rate of TF k_{TF} decreases. FIG. C1(c, d) show that the increase of singlet state decay rate k_{rad} accelerates the prompt FD, which is consistent with its physical interpretation. FIG. C1(e, f) show the effects of the combination rate k_{comb} and dissociation rate k_{dis} of triplet pair on fluorescence dynamics. k_{comb} and k_{dis} reflect the rates of two opposite processes, thus they have inverse effects on FD that are respectively similar to that of k_{SF} and k_{TF}. FIG. C1(g, h) show the effect of the hopping rate k_{h} of the single triplet excitons between neighbouring sites, in which the supplement of the hopping to singlet population prevents FD at later period. Particularly, the increase of k_{h} strengthens the singlet state decay and SF at any time as shown FIG. C1(g), but first impairs and then strengthens the total transition of singlet state after some critical point due to the competition between hopping of single triplet state excitons and decay of singlet state excitons as displayed in FIG. C1(h). We set the value of k_{h} that satisfies the relation $k_{\mathrm{h}} < k_{\mathrm{dis}}$ in order to be physically reasonable. FIG. C1(i, j) exhibit the effect of relaxation rate k_{relax} among the triplet pair states and separated triplet pair states. It can be seen in FIG. C1(i) that the increase of k_{relax} impairs the prompt fluorescence and strengthens the delayed fluorescence. The reason is that with k_{relax} increasing there is more population to be provisionally reserved.

ESI D: The MFEs comparison for different molecules in crystal structures

Rubrene crystals have 11 different polymorphs, which is dependent on the temperature, substrate, and the method to grow, and can be obtained by following several different routes [3, 4]. The polymorphs can be divided three classes, i.e., monoclinic, triclinic, and orthorhombic polymorph. The first two crystalline structures generate through solution crystallization methods [4], and the third structure generates through physical vapour growth [3]. In the three structural rubrene crystals, the molecular planes of two adjacent molecules are respectively perpendicular, parallel, and herringbone-packing to each other. The orthorhombic rubrene crystal is easy to obtain, even with sizes up to some centimeters and shows the best transport properties, in which the dihedral of two adjacent herringbone molecules is 61.4° [5]. In addition, in order to compare different molecules, we choose the tetracene and pentacene crystals that have 1 and 12 different polymorphs with different molecular arrangements referencing the U.S. National Library of Medicine. In herringbone tetracene crystal, the dihedral of two adjacent molecules is 51°. For herringbone pentacene, we choose one of the 12 polymorphs that is the thin film phase and is formed on the oxidized silicon substrates under high vacuum conditions, in which the dihedral of two adjacent molecules is 54.1° [6]. From the crystalline structures of the monoclinic, triclinic and orthorhombic rubrene, as well as herringbone tetracene and pentacene, it is clear that one of the two inequivalent molecules rotates 90°, 0° and 61.4° around y-axis, as well as 51° and 54.1° around x-axis, being overlapped with the other one, respectively. Their MFEs are shown in FIG. D1 in which the orientation of the applied magnetic field always is parallel with z-axis of molecule **a**. If their interaction strengths (including $g\beta$, D, E, and X) are approximately assumed to be the same, we can know according to the Fig. 1 and 2(e_2) in text that the MFEs on the FD of the triclinic and orthorhombic rubrene strengthen the prompt fluorescence and impair the delayed fluorescence, but on the monoclinic rubrene the magnetic field has the inverse impact. Hence, the FIG. D1

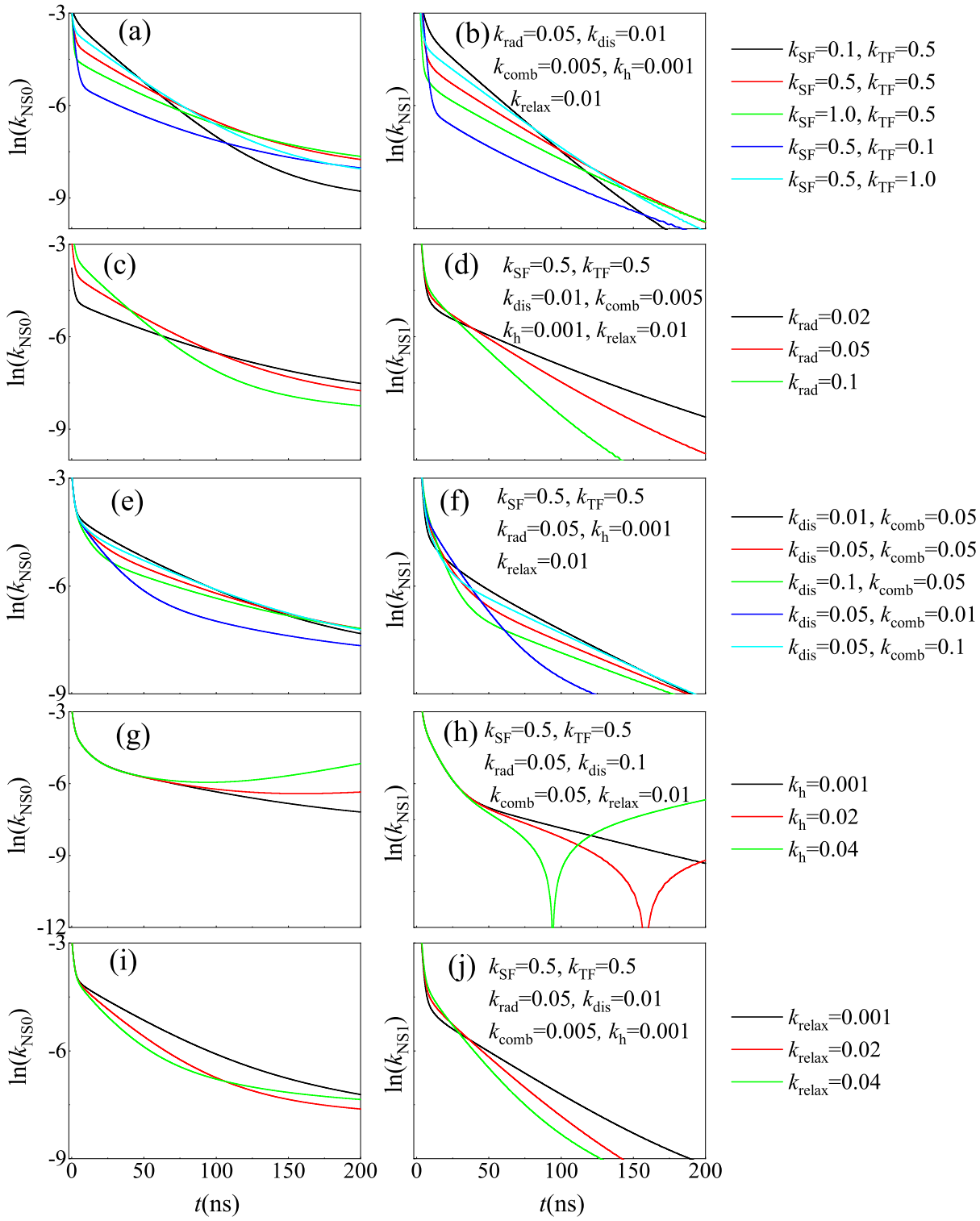

FIG. C1: (color online) The effects of the parameters $k_{SF,TF}$ (a,b), k_{rad} (c,d), $k_{dis,comb}$ (e,f), k_h (g,h), and k_{relax} (i,j) on FDs for magnetic random. The remainder parameters used are $B = 0.81$ T, $g\beta = 500$ m^{-1}T^{-1}, $D = -0.62$ m^{-1}, $E = 2.48$ m^{-1}, and $X = 0.01$ m^{-1}.

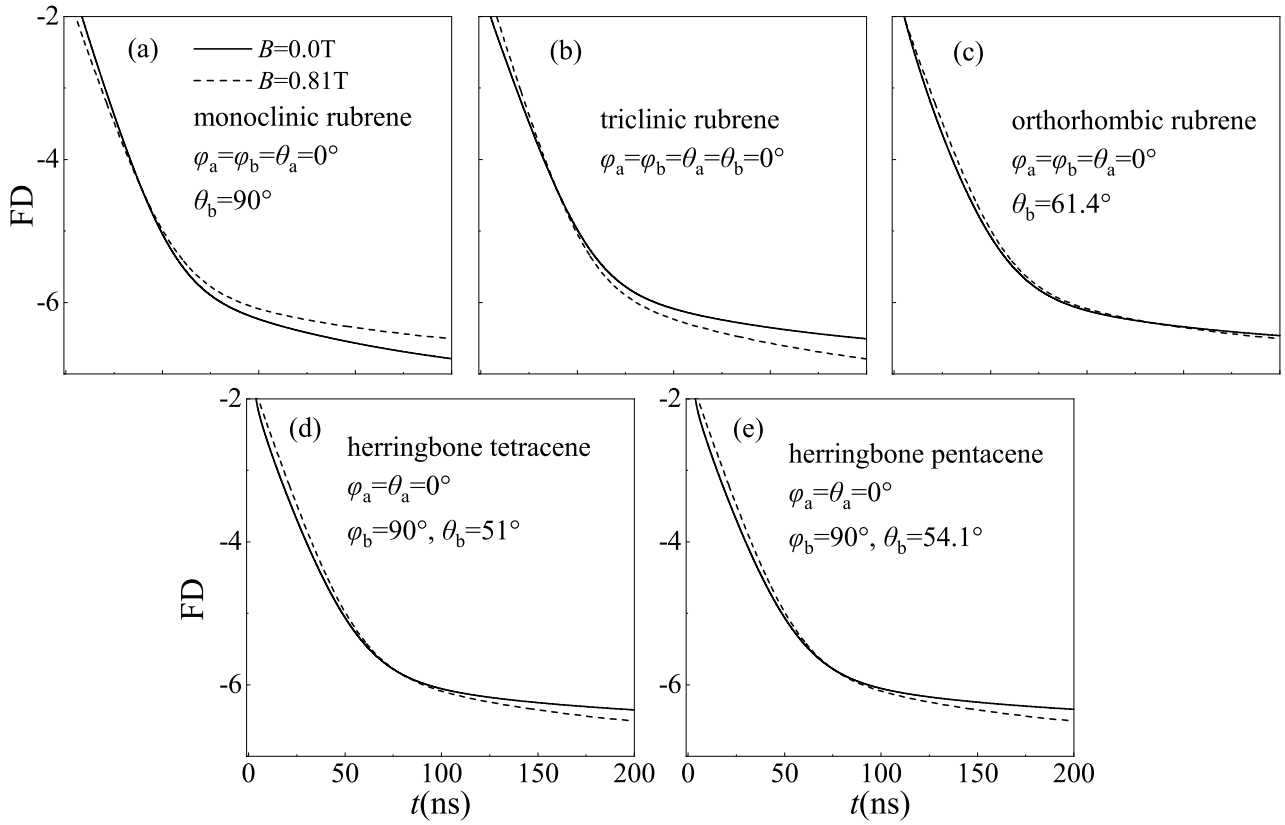

FIG. D1: The comparison about the different molecular MFEs on FD under the optimal rates fitted in the Fig. 5 of the text. The orientation of the magnetic field is parallel with z-axis of molecule **a**. The used parameters are $D = -0.62$ m^{-1} and $E = 2.48$ m^{-1} for rubrene and tetracene [1], $D = 3.05$ m^{-1} and $E = 0.79$ m^{-1} for pentacene [2], and the other parameters are $\gamma_b = 0°$, $g\beta = 500$ m^{-1}T^{-1}, and $X = 0.01$ m^{-1}.

shows that the MFE of the monoclinic rubrene [FIG. D1(a)] on FD is better than the others.

[1] L. Yarmus, J. Rosenthal and M. Chopp, *Chemical Physics Letters*, 1972, **16**, 477–481.
[2] O. Loboda, B. Minaev, O. Vahtras, B. Schimmelpfennig, H. Ågren, K. Ruud and D. Jonsson, *Chemical physics*, 2003, **286**, 127–137.
[3] O. D. Jurchescu, A. Meetsma and T. T. Palstra, *Acta Crystallographica Section B: Structural Science*, 2006, **62**, 330–334.
[4] L. Huang, Q. Liao, Q. Shi, H. Fu, J. Ma and J. Yao, *Journal of Materials Chemistry*, 2010, **20**, 159–166.
[5] S. M. Ryno, C. Risko and J.-L. Brédas, *ACS applied materials & interfaces*, 2016, **8**, 14053–14062.
[6] D. Nabok, P. Puschnig, C. Ambrosch-Draxl, O. Werzer, R. Resel and D.-M. Smilgies, *Physical Review B*, 2007, **76**, 235322.